miR-135b coordinates progression of ErbB2-driven mammary carcinomas through suppression of MID1 and MTCH2.

Arigoni M(1), Barutello G, Riccardo F, Ercole E, Cantarella D, Orso F, Conti L, Lanzardo S, Taverna D, Merighi I, Calogero RA, Cavallo F, Quaglino E.

miR-135b coordinates progression of ErbB2-driven mammary carcinomas through suppression of MID1 and MTCH2

Running title: miR135b and ErbB2^{+} mammary carcinoma

Maddalena Arigoni[*], Giuseppina Barutello[*], Federica Riccardo[*], Elisabetta Ercole[*], Daniela Cantarella[†], Francesca Orso[‡,§], Laura Conti[*], Stefania Lanzardo[*], Daniela Taverna[‡], Irene Merighi[*], Raffaele A. Calogero[*§,‖], Federica Cavallo[*] and Elena Quaglino[*]

[*]Molecular Biotechnology Center, University of Torino, Italy

[†]Institute for Cancer Research and Treatment, Department of Oncological Sciences, University of Torino, Candiolo, Italy

[‡]Molecular Biotechnology Center, Department of Oncological Sciences, University of Torino, Torino, Italy

[§]Center for Complex Systems in Molecular Biology and Medicine, University of Torino, Italy

[‖]Bioinformatics and Genomics Unit, University of Torino, Italy

Elena Quaglino and Federica Cavallo equally contributed

Number of text pages: 18

Number of tables: 1

Number of figures: 7

Running head: miR135b and ErbB2 mammary cancer

This work was supported by the Associazione Italiana per la Ricerca sul Cancro (AIRC, IG 5377); the Italian Ministry for the Universities and Research (PRIN 2008W3KW2A, PRIN , and FIRB giovani RBFR08F2FS-002 FO); the Regione Piemonte (Piattaforma innovativa "Biotecnologie per le scienze della vita", ImmOnc project); Epigenomics Flagship Project EPIGEN, MIUR-CNR.

Address correspondence to Raffaele A. Calogero, Molecular Biotechnology Center, Via Nizza 52, 10126 Torino, Italy. Phone: (0039)0116706457; Fax: (0039)0116706487; e-mail: raffaele.calogero@unito.it

Abstract

In an attempt to reveal deregulated miRNAs associated with the progression of carcinomas developed in BALB-neuT transgenic mice, we found increased expression of miR-135b during malignancy. Relevantly, we observed that miR-135b is up-regulated in basal or normal-like human breast cancers and it correlates with patient survival and early metastatization. Therefore, we investigated its biological functions by modulating its expression (up or down-regulation) in mammary tumor cells. While no effect was observed on proliferation in cell culture and in orthotopically injected mice, miR-135b was able to control cancer cell stemness in a mammosphere assay, anchorage-independent growth in vitro and lung cancer cell dissemination in mice following tail vein injections. Focusing on miR-135b molecular mechanism, we observed that miR-135b controls malignancy via its direct targets MID1 and MTCH2 as proven by biochemical and functional rescuing/phenocopying experiments. In line with this, an anti-correlation between miR-135b and MID1 or MTCH2 was found in human primary tumor samples. In conclusion, our research led us to the identification of miR-135b and its targets MID1 and MTCH2 as relevant coordinators of mammary gland tumor progression.

Breast cancer is one of the major health problems of the Western World.[1] Although the survival rate has improved with progress in screening and adjuvant therapies, one-third of the patients present cancer recurrences 10 years after the diagnosis.[2] More than 90% of mortality from cancer is attributable to metastases and not to the primary tumor from which metastases arise.[3] Identification of the genetic and epigenetic changes foreshadowing metastasis is thus one of the highest priorities for translational cancer research. While several protein-coding genes involved in malignancy have been identified and characterized,[4] non-coding-genes, such as microRNAs (miRNAs) that have been shown to regulate many aspects of the metastatic process have to be characterized.[5] Several clinical studies show a correlation between miRNA expression and recurrence, development of metastasis and/or survival.[6] miRNAs may also contribute to the metastatic program by modulating the structure of the tumor microenvironment influencing the ability of cancer cells to move and survive.[7] Moreover, miRNAs are involved in the maintenance of the cancer stem cell phenotype by connecting stemness and metastasis through regulation of epithelial-to-mesenchymal transition.[8] Global miRNA deregulation has been shown in breast cancer[9-12] while specific miRNAs have been associated with clinico-pathological features of breast tumors such as estrogen and progesterone receptor expression,[13] tumor grade,[10] vascular invasion or proliferation index.[14] As far as breast cancer is concerned, among other findings, reduced expression of miR-145,[15] miR-335,[16] and miR-126,[17] and over-expression of miR-10b,[18] miR-21,[19] and miR-210,[20] were significantly associated with breast cancer invasion and metastasis. However, profiling studies have been mainly focused on miRNAs deregulated in primary breast cancer[12, 21] or in breast cancer cell lines.[22] By contrast, characterization of a deregulated miRNA expression profile during carcinogenesis progression would permit to assess their involvement in tumor development and the efficacy of miRNA targeting during tumor progression.

BALB-neuT mice are a realistic model of mammary cancer, since all females develop invasive and metastatic rat ErbB2^{+} mammary carcinomas with a stepwise progression similar to that of

women.[23, 24] As in several cases of human mammary cancer, systemic metastatization is an early event in BALB-neuT carcinogenesis.[25] Moreover, gene expression pattern associated with cancer progression reveals major similarities with human ErbB2^{+} breast carcinomas.[26, 27] In this study, we show that miR-135a and miR-135b are strongly up-regulated in invasive carcinomas of BALB-neuT mice compared to normal mammary tissue. Down-modulation of miR-135b in cancer cells from BALB-neuT mice revealed its major role in anchorage-independent growth and lung metastasis formation. MID1 and MTCH2 were also identified and validated as putative miR-135b targets.

Materials and Methods

Mice

Female BALB/c and rat ErbB2 transgenic BALB-neuT mice[28] were bred by Biogem IRGS (Ariano Irpino, Italy), maintained in the transgenic unit of the Molecular Biotechnology Center (University of Torino) under a 12-hour light-dark cycle, and provided for food and water *ad libitum*. Mice were treated in conformity with European laws and policies,[29] and this study was approved by the Ethical Committee of the University of Torino.

Cell lines and mammosphere culture

BALB-neuT line 1(TUBO cells)[30], BALB-neuT line 2 and BALB-neuT line 3 are derived from autochthonous ErbB2^{+} mammary carcinomas arising in BALB-neuT female mice. They were cultured in DMEM with Glutamax 1 (Life Technologies) supplemented with 20% heat-inactivated FBS (Invitrogen) (complete medium). TSA (highly aggressive and metastatizing cell line established from a moderately differentiated mammary adenocarcinoma that arose spontaneously in a BALB/c mouse)[31] and 4T1 (mouse breast cancer cells sourced from American Type Culture Collection, Rockville, MD, USA) cell lines were maintained in RPMI (Life Technologies)

supplemented with 10% heat-inactivated FBS (Invitrogen). TUBO, TSA and 4T1 cells were grown in adherent conditions as epithelial monolayer in mammosphere medium (serum-free DMEM-F12 medium supplemented with 20 ng/ml basic-fibroblast growth factor, 20 ng/ml epidermal growth factor, 5 μg/ml insulin, and 0.4% bovine serum albumin, all from Sigma-Aldrich) to generate E cells.

TUBO cells were dissociated enzymatically and mechanically, using trypsin and pipetting, and were plated in ultra-low attachment flasks (Corning Life Sciences) at 6 x 10^4 viable cells/ml in mammosphere medium, as previously described.[32] Non-adherent spherical clusters of cells, named P1, were collected by gentle centrifugation after 7 days and disaggregated through enzymatic and mechanical dissociation. The cells were analyzed microscopically for single-cellularity and seeded again at 6 x 10^4 viable cells/ml to generate non-adherent spherical clusters of cells, named P2.

RNA isolation and qRT-PCR (qPCR) for mRNA and miRNA detection

Total RNA was isolated from cells, mammospheres and from the II, III and IV right mammary glands of mice bearing diffused atypical hyperplasia (six weeks of age) and invasive lobular carcinomas (nineteen weeks of age) using the *mir*VanamiRNA isolation kit (Applied Biosystems). RNA was estimated qualitatively with Agilent 2100 Bioanalyzer (Agilent Technologies) and quantified with NanoVuePlus Spectrophotometer (GE Healthcare). Total RNA was stored at -80°C till used. qPCRs for miRNA detection were performed with TaqMan® MicroRNA Assays (Applied Biosystems) on 10 ng total RNA following manufacturer's instructions. For mRNA detection, 1 μg of DNase-treated RNA (DNA-free™ kit, Ambion) was retrotranscribed with RETROscript™ reagents (Ambion) and qPCRs were carried out using gene-specific primers (QuantiTect Primer Assay,Qiagen), SYBR green (Applied Biosystems) and 7900HT RT-PCR System (Applied Biosystems). Quantitative normalization was performed on the expression of sno-412, U6 or β-actin for miRNAs or mRNA detection respectively. The relative expression levels between samples were calculated using the comparative ΔCt method[33].

qPCR low density miRNA arrays

Four conditions were investigated using Applied Biosystems Megaplex low density qPCR miRNA expression arrays: 19-weeks-old BALB-neuT and BALB/c (wk19.neu, wk19.BALB/c), 6-weeks-old BALB-neuT and BALB/c (wk6.neu, wk6.BALB/c) mice. Two animals were analyzed for each condition. qPCR runs were performed by technical support of Applied Biosystems Italia. Raw Ct data were analyzed using Bioconductor.[34] 259 probes out of 381 were left after removal of non-informative probes (those with Ct > 35 in 6 out of 8 samples). ΔCts were calculated with respect to the mammalian U6 endogenous control. Data are available at http://www.bioinformatica.unito.it/quaglino.et.al/. Using rank product method,[35] differential expression was calculated between wk19.neu and wk19.BALB/c, between wk6.neu and wk6.BALB/c, and between wk19.neu and wk.6.neu. This method addresses the multiple comparison problem and performs p-value correction by false-discovery-rate (FDR), comparing the true rank product distribution with a random one defined permuting miRNA labels in each of the cards under analysis. Here, we have used 1000 permutations and a threshold of percentage of false positive predictions (pfp) of 0.05.

RNA-seq for miRNAs

Mammary glands from two wk19.BALB/c and two wk19.neu were evaluated. 1.5 μg of total RNA was used forSOLiD short RNA library preparation following manufacturer's instructions (Applied Biosystems). Library preparation and sequence data generation were provided as service by Genomnia Srl. SOLiD v3 sequence data in color space, 35 color calls, were cleaned[36] and trimmed at 25 color calls to remove the P2 linker. Reads mapping was done on the subset of ENSEMBL non-coding RNA (miRNA, rRNA, tRNA, snoRNA, snRNA) using SHRIMP software[37] with the following parameter: -n 1; -w 170%; -M miRNA; -o 1. SHRIMP outputs were reformatted and imported into oneChannelGUI.[38] Differential expression analysis on counts data (available at

http://www.bioinformatica.unito.it/quaglino.et.al/) was done using negative binomial dispersion[39] implemented in the edger Bioconductor package (threshold $P \leq 0.05$).

miR-135b meta-analysis of human breast cancers

The associations between miR-135a and miR-135b expression and survival and or distant metastasis relapse were assessed using two datasets[12, 21] encompassing both miRNA and mRNA expression. For both these datasets available on GEO (GSE19536, GSE22220) the expression data of miR-135a and miR-135b were extracted together with survival information. K-mean clustering (k = 2) was used to cluster samples in two groups: set of samples characterized by the highest miR-135a and miR-135b average expression level (high) and set of samples characterized by the lowest miR-135a and miR-135b average expression level (low). Cox proportional hazards regression model was fitted to survival data for high and low groups in the two datasets.

Enerly data set was also used to search for anti-correlation between miR-135b and its targets MID1 and MTCH2. Samples were stratified on the basis of subgroups as defined by Perou et al.[40] Linear regression was used to measure and quantify anti-correlation between miR-135b and MID1 and MTCH2 expression data using the Spearman's rank correlation test. Values between 0 and -1 indicates the presence of anti-correlation while values between 0 and +1 indicates the presence of correlation.

Transient cell transfection

To obtain adherent TUBO or P1 derived cells silenced or overexpressing miR-135b, 3 x 10^5 or 1.2 x 10^5 cells/well in 6-well plates respectively, were transfected using Lipofectamine 2000 (Invitrogen) with 200 nM of miR-135b miRIDIAN Hairpin Inhibitor (anti-miR-135b antagomir) or 100 nM of miR-135b miRIDIAN Mimics (miR-135b mimic) (Dharmacon). For each experiment cells were also transfected with miRIDIAN microRNA Hairpin Inhibitor (scrambled antagomir) or

Mimics (scrambled mimic) negative controls. Cells were tested for miR-135b knockdown or over-expression 24, 48 and 72 h after transfection.

To demonstrate a causal role of MID1 and MTCH2 downstream of miR-135b, a rescue experiment was performed by transfecting TUBO cells using Lipofectamine 2000 (Invitrogen) with 10 μg of plasmids containing the cDNA of MID1 or MTCH2 genes without 3'UTR (Gene-Copoeia) and thus miR-135b insensitive. pVAX empty plamid was used as control. Forty-eight h later, TUBO cells were transfected with 100 nM of miR-135b miRIDIAN Mimics. Twenty-four h later, 5 x 10^4 TUBO cells from each experimental condition were assayed in triplicate for their ability to growth in an anchorage-independent conditions. At the same time, RNA was isolated from transfected cells to test miR-135b, MTCH2 and MID1 expression.

To obtain the phenocopy of miR-135b over-expression, knockdown of MID1 target gene was obtained by transfecting 3 x 10^5 TUBO cells with 200 nM of specific siRNA or non targeting siRNA as control (ON-TARGET plus SMART pool siRNA, Dharmacon).

Flow cytometry analysis

TUBO, P1, P2 and P1 cells 24 h after transfection were collected, disaggregated using enzymatic and mechanical dissociation, washed in PBS supplemented with 0.2 % BSA and 0.01 % sodium azide (Sigma-Aldrich). Cell suspensions were either stained for membrane antigens or fixed and permeabilized with the Cytofix/Cytoperm Fixation/Permeabilization Kit (BD Biosciences, Buccinasco, Milan, Italy) and then stained for intracellular antigens. The following antibodies (Ab) were used; Alexa Fluor647-conjugated anti-Stem Cell Antigen (Sca)-1, allophycocyanin (APC)/Alexa Fluor780-conjugated anti-Thy1.1 from Biolegend (London, UK), Alexa Fluor647-conjugated anti–Nanog mAb from eBioscience (Hatfield, UK). Samples were collected and analyzed using a CyAn ADP Flow Cytometer and Summit 4.3 software (DakoCytomation).

Sphere generation assay

TUBO cells were cultured at a density of 6 x 10^4 cells/ml in a six-well ultra-low attachment plate in the mammosphere medium. After five days of culture, P1 derived cells were transfected with anti-miR-135b antagomir or scrambled antagomir. Five days after transfection total number of mammospheres for each well was counted and reported as number of mammospheres generated for every 10^3 cells plated.

Anchorage-independent growth assays

Twenty four h after transfection 5 x 10^4 TUBO cells were suspended in complete medium containing 0.45 % Difco Noble Agar (Becton Dickinson), and plated in 6 cm bacterial dishes. Medium was changed every 3 days. 15 days later the dishes were stained with nitrobluetetrazolium (Sigma-Aldrich), and photographed with a Nikon SMZ1000 stereomicroscope. Colonies were counted with the ImageJ software (http://rsbweb.nih.gov/ ij/).

Total cell count assay

Twenty-four h after transfection, TUBO cells were plated at 5 x 10^3 cells/well in 96-well plates in DMEM and starved for 24 h. Complete medium was then added and cells were allowed to grow for 1-4 days, fixed with 2.5% glutaraldehyde, and stained with 0.1% crystal violet. The dye was solubilized using 10% acetic acid. Optical density was measured with a Microplate Reader 680 XR (Biorad) at 570 nm wavelength.

In vivo tumor growth and metastasization

Seven-week-old BALB/c female mice were challenged in the mammary pad with 1 x 10^5 TUBO cells. This pad was inspected weekly by palpation. Progressively growing masses > 1 mm in diameter were regarded as tumors. Mice were sacrificed when one tumor exceeded 10-mm mean diameter. For experimental metastasis assays, 2.5 x 10^4 TUBO, 5 x 10^4 TSA or 4T1 cells were injected into the tail vein of 7-week-old female BALB/c mice. Mice were sacrificed 20 days later

and total lungs were formalin-fixed, cut in small pieces, paraffin-embedded, sectioned and haematoxylin & eosin (H&E)-stained. Micrometastases were evaluated using an Olympus BH2 microscope, on three or more sections by using the ImageJ software.

miR-135b targets identification

Detection of miR-135b targets was done downloading from Miranda database (http://www.microrna.org) all those characterized by an optimal or sub-optimal miRSVR score,[41] and retaining only those with a human orthologue (ftp://ftp.informatics.jax.org/pub/reports/index.html#orthology). The expression of these genes was than evaluated by transcriptome analysis (MOUSEREF-8 V2 Illumina bead chips, GSE28949) in anti-miR-135b or scrambled transfected TUBO cells at 24, 48, and 72 h after transfection. Each experimental condition was repeated three times. cRNA synthesis and labeling were done with the Illumina RNA Amplification Kit (Ambion) following manufacturer's suggestions. Arrays were scanned on an Illumina BeadStation 500. Genome studio (Illumina) was used to generate a raw intensity signal without normalization. Data $\log_2$ transformation and loess normalization were performed with oneChannelGUI.[38]After removal of unchanging and not expressed genes by IQR filtering[42] (only genes with an IQR > 0.25 were retained), and linear model analysis[43] of differential expression, genes characterized by an uncorrected P-value < 0.05 and up-regulated in anti-miR-135b as compared to scrambled transfected TUBO cells were considered for further analysis.

Luciferase assay

3 x 10^5 TUBO cells were plated on a 6-well plate and 24 h later co-transfected using Lipofectamine2000 (Invitrogen) with 200 nM of anti-miR-135b or 100 nM of miR-135b mimic with 1 μg of pEZX-MT01 vector (Gene-Copoeia) containing firefly luciferase gene, the 3'UTR of the indicated miR-135b potential target genes, and renilla luciferase as tracking gene. Lysates were

collected 72 and 96 h after transfection and firefly and renilla luciferase activities were measured with a dual Luciferase Reporter System (Promega).

Protein preparation and Immunoblotting

Total protein extracts were obtained from transfected TUBO cells by using a boiling buffer containing 0.125 M Tris/HCl, pH 6,8 and 2.5 % sodium dodecyl sulphate (SDS). Protein level evaluation of MID1 and MTCH2 was performed on total lysates collected 72 or 48 h after transfection respectively. 30 μg proteins were separated by SDS-PAGE and electroblotted onto polyvinylidene fluoride membranes (BioRad, Hercules, CA). Membranes were blocked in 5 % Blotto non-fat milk (Santa Cruz, CA) Tris buffered saline (TBS)-Tween buffer (137 mM NaCl, 20 mM Tris/HCl, pH 7.6, 0.1 % Tween-20) for 1 h at 37° C, then incubated with appropriate primary and secondary antibodies in 1 % milk TBS-Tween buffer, overnight at 4° C and for 1 h at room temperature respectively, and visualized by enhanced chemiluminescence (ECL®, Amersham Biosciences, Piscataway, NJ). The anti-MTCH2 rabbit polyclonal antibody was from ProteinTech; the anti-MID1 rabbit polyclonal antibody was from LSBio; anti-actin mouse monoclonal antibody, goat anti-mouse IgG HRP-conjugated, goat anti-rabbit IgG HRP-conjugated antibodies were all from Santa Cruz. Protein modulations were calculated relative to controls, normalized on the actin loading control and expressed as percentages by using Quantity One software.

Results

Differential miRNA expression in invasive carcinoma and in normal tissue during ErbB2 mammary carcinogenesis

To assess a correlation between deregulation of miRNAs and breast cancer, miRNA profiling was performed in BALB-neuT mice.[24, 28] Previous observations[44] showed that changes in the composition of mRNA species associated with modification of the cell composition of the

mammary microenvironment can be used to tag tumor/microenvironment-associated genes. In this paper we used this approach to identify tumor-associated miRNAs. Two prototypic conditions of autochthonous carcinogenesis were investigated: diffused atypical hyperplasia present in the mammary glands of wk6.neu and invasive lobular carcinomas displayed by mammary glands of wk19.neu. Wild type mammary glands from age matched BALB/c animals (wk6.BALB/c and wk19.BALB/c) were included to take into account miRNAs changes due to physiological changes of the mammary glands. Transcription profiling was performed using Real-time PCR low density miRNA arrays. Principal component analysis (PCA) shows that miRNA profile changes are mainly linked to animal age (Figure 1, gray versus black circles). However, some differences were observed between atypical hyperplasia and invasive carcinoma when they were compared to age-matched normal mammary tissue (Figure 1, open versus closed circles). Rank product statistics[35] did not disclose significant differences in miRNA expression of hyperplasia versus age-matched normal mammary tissue (wk6.neu versus wk6.BALB/c). In contrast, two tumor associated miRNAs (mmu-miR-135a and mmu-miR-135b) were differentially expressed between lobular carcinoma versus age-matched normal mammary tissue (wk19.neu versus wk19.BALB/c). Their expression was confirmed in the mammary glands of 19-weeks-old BALB/c and BALB-neuT mice by qPCR on independent samples. No differences in the expression level were observed comparing wk6.BALB/c with wk6.neu for both miR-135a and miR-135b while a statistically significant increase was observed comparing wk19.BALB/c with wk19.neu (Figure 2). Furthermore, while miR-135a and miR-135b expression level was comparable between wk6.BALB/c and wk19.BALB/c (Figure 2A and B, white open circles), a statistically significant expression increment was found comparing wk6.neu with wk19.neu (Figure 2A and B, black closed circles), suggesting a correlation between miRNA expression and tumor mass increase. RNA-seq quantitative analysis performed on independent samples displayed a statistically significant increment only for miR-135a and miR-135b in wk19.neu as compared to that measured in wk19.BALB/c (miR-135a $\log_2$ fold change: 3.19 FDR < 0.05; miR-135b: $\log_2$ fold change: 4.36

FDR < 0.05). RNA-seq data were also used to evaluate miR-135a and miR-135b absolute concentration. Their ranking in wk19.BALB/c and in wk19.neu showed that they move from the bulk of low-expressed miRNAs (> 200 miRNAs) to a subgroup with medium expression (~ 60 miRNAs) (Supplemental Figure S1 at http://ajp.amjpathol.org).

miR-135a and miR-135b in human cancers

Very little is known about the association of miR-135a and miR-135b with human breast cancer.[13, 14] However, Blenkiron's[10] data sets performed on 93 primary human breast tumors highlighted that miR-135b is up-regulated in basal and normal-like breast cancer subgroups[40]. Moreover, Enerly's[12] data sets on 101 primary human breast tumors confirmed the over-expression of miR-135b in basal like tumor subtypes. Genome-wide investigations of miRNA status in primary human breast cancers done by Enerly and coworkers,[12] and by Buffa and coworkers,[21] are valuable tools to investigate the association between miRNA expression and patients' survival or distant metastasis relapse, respectively. Using this data and applying a Cox proportional hazards regression model, a statistical association between miR-135b up-modulation and poor survival ($P = 0.04$) was observed (Supplemental Figure S2 A at http://ajp.amjpathol.org), however no correlation with late (i.e. 120 months) distant metastasis was revealed (Supplemental Figure S2 B at http://ajp.amjpathol.org). Nevertheless, up-modulation of miR-135b seems to be involved in early (i.e. 50 months) distant metastasis relapse (Supplemental Figure S2 C at http://ajp.amjpathol.org). miR-135a expression does not show any significant association with patients' survival and distant metastasis appearance (not shown).

miR-135b does not affect in vitro and in vivo BALB-neuT tumor cell line proliferation

The over-expression of miR-135b in invasive mammary tumors of BALB-neuT mice, together with its correlation with poor survival in breast cancer patients, prompted us to explore its role in tumor cell proliferation. qPCR performed on three cell lines derived from BALB-neuT mammary tumors

and on two other unrelated BALB/c mammary tumor cell lines (TSA[31] and 4T1) showed that miR-135b was expressed in all tested cell lines even if at lower level in both TSA and 4T1 cells as compared to BALB-neuT tumor cells (Supplemental Figure S3 at http://ajp.amjpathol.org). The consequences of miR-135b deregulation were investigated in BALB-neuT line 1 (TUBO cells), in TSA and in 4T1 cells. qPCR analysis 72 h after transfection showed that miR-135b expression was almost completely abrogated when TUBO, TSA and 4T1 cells were transfected with specific antisense inhibitors (anti-miR-135b) and strongly up-regulated after its transient over-expression by specific mimics (miR-135b-over) (data not shown). By contrast, miR-135b expression was not affected after transfection with negative controls (scrambled). Both down-regulation and over-expression of miR-135b had a marginal effect on TUBO total cell count (Figure 3): only 10-15 % reduction of total cell number was observed in anti-miR-135b as compared to scrambled TUBO cells (Figure 3A), and 5-20 % enhancement of total cell number in miR-135b-over as compared to scrambled TUBO cells (Figure 3B). Comparable results were observed when miR-135b deregulation was studied on both TSA and 4T1 cells (data not shown). When TUBO cells in which miR-135b was silenced or overexpressed were injected subcutaneously in the flank of BALB/c mice, only a marginal effect on tumor incidence was observed (Figure 3C and D), while tumor growth speed was not affected at all (data not shown).

miR-135b is involved in cancer stem cells (CSC) self-renewal

Since miRNAs are involved in cancer stem cell phenotype maintenance by connecting stemness and metastasis,[8] an in vitro cultivation system that allows propagation of mammary epithelial TUBO cells in suspension as non-adherent mammospheres,[32] has been used to asses miR-135b level of expression in TUBO cell-derived non adherent mammospheres and in differentiated mammary TUBO cells. FACS analysis of some stem cell markers showed that the percentage of Sca-1[32], Thy1.1 [45] and Nanog [46] positive cells significantly increased progressively from TUBO to P1 and P2 passages of mammospheres (Figure 4A). Level of miR-135b was significantly higher in P1 and

P2 mammospheres compared with that of differentiated TUBO cells (Figure 4B). Similar results were observed when miR-135b expression was assessed in mammospheres from TSA (Supplemental Figure S4 at http://ajp.amjpathol.org). To further analyze miR-135b involvement in CSC self-renewal, P1 mammospheres where transfected with anti-miR-135b or scrambled antagomir and sphere generation was evaluated. As reported in Figure 4C, miR-135b silencing significantly reduced mammosphere generation in a sphere generation assay. This inhibition is associated with a reduction in the percentage of Sca-1, Thy1.1 and Nanog expressing cells (Figure 4D).

miR-135b over-expression enhances colony formation in vitro and metastasis formation in vivo

Enerly'[12] and Buffa's [21] meta-analysis suggest a correlation between miR-135b over-expression in breast cancer and poor survival and early metastases relapse. We thus looked to see whether miR-135b has any activity linked to metastasis formation in BALB-neuT mammary cancer cells. Anchorage-independent growth in soft agar was evaluated by both silencing and overexpressing miR-135b in TUBO cells. Anti-miR-135b TUBO cells cultured in soft agar show a significant reduction in the number of colonies as compared to those observed with scrambled TUBO cells (98.3 ± 14.4 versus 203.0 ± 9.5 colonies, $P = 0.004$) (Figure 5A), whereas a significant enhancement of the number of colonies was observed in miR-135b-over as compared to scrambled TUBO cells (148.7 ± 12.1 versus 96.5 ± 10.4 colonies, $P = 0.02$) (Figure 5B). Because of its ability to enhance anchorage-independent growth, we also investigated whether miR-135b influences metastasis formation in vivo. Thus, anti-miR-135b or miR-135b-over TUBO cells were injected into the tail vein of BALB/c mice and lung micrometastasis were counted. Anti-miR-135b TUBO cells were significantly ($P = 0.02$) less able to seed and formed fewer lung metastases than the scrambled TUBO cells (Figure 5C). In contrast, significantly ($P = 0.01$) more lung metastases were observed for miR-135b-over when compared with scrambled TUBO cells (Figure 5D). Up-regulation of miR-135b in both TSA and 4T1 cells resulted in an increase of the number of lung

metastases when injected in BALB/c mice, suggesting a role of miR-135b in tumor metastatization also in these tumor cell lines (Supplemental Figure S5 at http://ajp.amjpathol.org).

miR-135b target genes

The first step in the detection of miR-135b targets was the extraction of all predicted mouse miR-135b targets (3888 genes) from the Miranda database (http://www.microrna.org), retaining only those having a human orthologue (1054 genes). The following step was to evaluate their differential expression in anti-miR-135b or in scrambled TUBO cells 72 h after transfection by Illumina microarrays. Importantly, qPCR data showed that miR-135b expression reached nearly 100 % of reduction only at 72 h (Supplemental Figure S6 at http://ajp.amjpathol.org). The 17 genes up-regulated in anti-miR-135b TUBO cells were considered as putative miR-135b targets (Table 1). Since down-regulation of two of them only (MID1 and MTCH2) was known to be associated to a more aggressive phenotype in solid tumors,[47, 48] we focused our attention on them.

To determine whether MID1 and MTCH2 are bona fide targets of miR-135b, two reporter vectors with MID1 and MTCH2 3'UTR fragments containing the miR-135b binding sequences (Supplemental Figure S7 at http://ajp.amjpathol.org), were used to perform luciferase assays. As shown in Figure 6A, luciferase expression driven by the 3'UTRs of MID1 and MTCH2 was significantly enhanced in anti-miR-135b as compared to scrambled TUBO cells. Consistent with the luciferase and the genome wide microarray analysis results, MID1 and MTCH2 mRNA levels measured by qPCR were significantly enhanced in anti-miR135b TUBO cells as compared to those in scrambled TUBO cells. Modulation of MID1 and MTCH2 mRNA corresponded to fluctuations of MID1 and MTCH2 protein level (+ 10 % and + 20 % respectively) in anti-miR-135b as compared to those measured in scrambled TUBO cells (Figure 6C). Moreover following miR-135b over-expression in TUBO cells was associated with a decrease of MID1 and MTCH2 protein levels(- 93 % and - 23 % respectively) (Figure 6C). We than investigated the possible direct regulation of MID1 and MTCH2 by miR-135b in vivo, by comparing their mRNA expression

during BALB-neuT mammary tumor progression. A significant reduction in mRNA of MID1 and MTCH2 was observed in wk19.neu vs wk6.neu mammary glands (Figure 6D).

To evaluate whether the prometastatic effect mediated by miR-135b is MID1 or MTCH2 dependent, we measured the anchorage independent colony formation ability of miR-135b over-expressing TUBO cells also expressing MID1 or MTCH2 coding sequences lacking the 3' UTR, therefore yielding a product resistant to miR-135b mediated suppression. miR-135b mimic transfected TUBO cells over-expressing MID1 or MTCH2 miR-135b insensitive cDNA show a significant reduction of colony formation ability as compared to that measured in miR-135b mimic TUBO cells transfected also with the empty plasmid (Figure 7). In addition, to further confirm the direct link between MID1 and colony formation ability of TUBO cells, a phenocopy experiment of miR-135b over-expression was performed by silencing MID1 target gene with specific siRNA. A significant higher number of colonies was observed after MID1 knocking-down (Supplemental Figure S8 at http://ajp.amjpathol.org). Taken together, these data indicate that the down-regulation of MID1 and MTCH2 by miR-135b is the mechanism by which miR-135b promotes anchorage independent progression of ErbB2-driven mammary carcinomas.

Taking advantage of the available data on miRNA status and mRNA transcription profile of published by Enerly and co-workers[12], we looked for the presence of an anti-correlation between miR-135b expression and MID1 or MTCH2 modulation in primary human breast cancers. Since miR-135b is significantly up-modulated only in basal and normal-like breast cancer subtypes as shown by Blenkiron and co-workers,[10] we stratified the mRNA data on the basis of the clinical annotation available for the Enerly data set. A clear anti-correlation between miR-135b and MID1 and MTCH2 was found in the subset of tumors defined as normal-like (Supplemental Figure S9 at http://ajp.amjpathol.org), reinforcing the relevance of miR-135b and its targets in breast tumorigenesis.

Discussion

Over the last 10 years, miRNAs have attracted attention on account of their ability to post-transcriptionally modulate the expression of oncogenes and oncosuppressors. Several reports have described their involvement in the initiation and progression of most cancers. miRNAs overexpressed in tumors contribute to oncogenesis by deregulating tumor suppressors, whereas miRNAs lost by tumors participate in oncogene over-expression. Notably, roles of miRNAs in cancer are tissue and tumor specific, and alterations in miRNA expression alone can cause cell neoplastic transformation.[49] In addition, a specialized family of miRNAs (metastamir) modulate the metastatic behavior of neoplastic cells[50] and is involved in the regulation of the epithelial-mesenchymal transition.[51] miRNAs may also contribute to the metastatic program by both modulating the structure of local tumor microenvironment, and by promoting neo-angiogenesis during tumor progression.[52]

The mutated form of rat ErbB2 oncogene drives an aggressive mammary carcinogenesis in BALB-neuT mice. The steps of this progression mimicking a few features of human breast tumors[23] have been extensively characterized at the transcriptional level.[53-55] The analysis of miRNA expression reported here shows an increased expression of miR-135a and miR-135b during tumor expansion in function of the mouse age. The decreased expression of these two miRNAs observed in function of the age in the mammary glands of normal mice endorses their involvement in tumor development. Little is known about the expression of these two miRNAs in tumors. miR-135a down-regulation has been associated with the anti-cancer effect of mistletoe lectin-I[56] and with a higher probability of relapse in classic Hodgkin lymphoma patients.[57] Recently miR-135a and miR-135b up-modulation has been shown to correlate with the degree of malignancy in colon cancer,[58-60] in osteosarcoma,[61] in ependymoma,[62] and in hepatocellular carcinoma.[63] While miR-135a and miR-135b involvement in breast cancer has never been described, by exploiting data on the expression of miRNAs in human breast cancers[12, 21], the over-expression of miR-135b, but not miR-135a, appeared to be associated with poor prognosis. In addition, miR-135b over-expression in basal-like and estrogen-negative human tumor shown by this meta analysis fits in well with the notion that

mammary tumors of BALB-neuT mice are similar to basal-like and estrogen-negative human mammary carcinomas.[26]

TUBO cells were established from a BALB-neuT mammary carcinoma.[64] As expected, since TUBO cells are ErbB2-addicted, miR-135b expression was not strictly involved in promoting their proliferation, neither in vitro, nor in vivo, but was associated with their anchorage-independent growth and to their ability to give rise to lung metastasis. Moreover, expression of miR-135b increases in non-adherent spherical clusters of different breast cancer cell lines, that display increased tumorigenic and metastatic ability.[32] Furthermore, miR-135b involvement in cancer stem cell phenotype maintenance is demonstrated by the significant reduction of mammospheres after its silencing in P1 derived TUBO cells.

To investigate the molecular mechanism underlying the miR-135b's functionality, we searched for its targets, since their computational prediction is essential for elucidating the detailed functions of miRNA. However, the specificity and sensitivity of the existing algorithms are still too poor to generate meaningful, workable hypotheses for subsequent experimental testing.[65] Integration of prediction with other experimental methods investigating target modulation are thus required to improve target detection specificity. Although miRNAs only partially suppress gene expression and promote mRNA decay, a certain effect at the level of target mRNA concentration can be detected with carefully designed microarray experiments.[66] Combining target prediction knowledge derived from miRanda with a gene expression profile experiment, in which we look for up-regulated genes after miR-135b silencing in TUBO cells, we detected seventeen putative targets. However, among all these genes only MID1 and MTCH2 expression was associated with a statistical significant up-regulation 72 h following miR-135b silencing in TUBO cells, suggesting a direct link to this miRNA. Moreover, MID1 and MTCH2 down-modulation in tumor cells has been reported to be associated to a more aggressive phenotype being part of a gene signature associated with metastasis and survival in solid tumors.[47, 48] MID1 forms homodimers which associate with microtubules in the cytoplasm, and is probably involved in the formation of multiprotein structures acting as anchor

points for microtubules.[67] MTCH2, also called Met-induced mitochondrial protein[68], is an outer mitochondrial membrane protein whose induction cause growth and motility arrest in vitro, loss of tumorigenicity in vivo[68] and, facilitate apoptosis.[69] The luciferase assay showed that both are bona fide miR-135b targets. The role of miR-135b in the anchorage-independent cells growth and the fact that MID1 and MTCH2 down-regulation is associated with increased invasiveness in both BALB-neuT mice and in solid human cancers,[47, 48] points to a role of miR-135b in invasion and metastasis formation in breast cancer. Moreover, the presence of an anti-correlation between miR-135b and MID1 and MTCH2 expressions in human breast cancer specimens of normal like subtype, highlighted the relevance of the whole study for the understanding of human breast cancer.

The detection of the role of miR-135b in BALB-neuT mammary carcinogenesis provides a well characterized preclinical model for exploration of the potentiality of miR-135b, MID1, and MTCH2 as new therapeutic targets.

Table1. miR-135b putative targets

Probe ID	EG*	Symbol	Log_2 FC†	Average intensity‡	P value
ILMN_1238032	242960	FBXL5	0.73	9.87	0.001
ILMN_1244768	20818	SRPRB	1.12	10.35	0.002
ILMN_2619452	17318	MID1	0.54	8.38	0.003
ILMN_2718612	68291	MTO1	0.56	9.37	0.004
ILMN_2654568	72133	TRUB1	0.71	9.13	0.007
ILMN_2914271	11836	ARAF	0.82	11.32	0.010
ILMN_2755981	226151	FAM178A	0.97	10.11	0.011
ILMN_2610204	56428	MTCH2	0.64	9.52	0.011
ILMN_2710705	18412	SQSTM1	0.89	12.36	0.015
ILMN_2668387	106143	CGGBP1	0.59	11.39	0.020
ILMN_2737296	102436	LARS2	0.41	9.28	0.022
ILMN_1229418	12807	HPS3	0.56	8.99	0.022
ILMN_1226187	14768	LANCL1	0.72	9.82	0.023
ILMN_3009880	242700	IL28RA	0.36	8.78	0.024
ILMN_1258977	67878	TMEM33	0.78	11.28	0.039
ILMN_1225723	72085	OSGEPL1	0.45	9.36	0.042
ILMN_2757150	18555	PCTK1	0.50	10.01	0.047

*Entrez gene ID, †Log_2 fold change variation , ‡Log_2 average fluorescence intensity

The above 17 genes were obtained by the intersection of genes detected as up-regulated upon miR-135b silencing ($P \leq 0.05$) and the putative target of miR-135b extracted from Miranda database

Figure Legends

Figure 1. Principal component analysis (PCA) of global miRNA expression changes. Transcription profiling of mammary gland samples from 6-week old BALB-neuT (wk6.neu), 19-week old BALB-neuT (wk19.neu) and age matched wild type BALB/c (wk6.BALB/c and wk19.BALB/c) mice was performed using Applied Biosystems Real-time PCR low density miRNA arrays. (**A**) PCA analysis. miRNA expression profile changes are mainly linked to animal age, however that of invasive carcinoma is different from that of age-matched normal mammary tissue (black closed versus white open circles) while that of atypical hyperplasia and normal tissue is more similar (gray closed versus white open circles). (**B**) Amount of variance explained by each of the PCA components.

Figure 2. miR-135a (**A**) and miR-135b (**B**) expression levels measured in the mammary glands of 6 and 19-week-old BALB/c (white open circles) and BALB-neuT (black closed circles) mice measured by qPCR. Each dot represents the evaluation of miRNA levels in a single mouse. ΔCts were calculated with respect to the mammalian sno-412 RNA level. Statistically significant differences were calculated using the Student's t test (wk6.BALB/c versus wk19.BALB/c $P = 0.01$ for miR-135a; wk.6neu versus wk19.neu $P < 0.0001$ for miR-135a and miR-135b; wk19.BALB/c versus wk19.neu $P < 0.0001$ for miR-135a and $P < 0.001$ for miR-135b).

Figure 3. miR-135b expression does not significantly affect tumor cell growth both in vitro and in vivo. TUBO cells were transfected with a specific miR-135b antisense inhibitor (anti-miR-135b) or mimic (miR-135b-over) or their negative controls (scrambled). (**A, B**) TUBO cells proliferation was evaluated 24, 48, 72 and 96 h after down-regulation (**A**) or over-expression (**B**) of miR-135b. Three independent experiments (at least in quadruplicate) were performed and a representative one is shown as mean ± SEM. (**C, D**) miR-135b effect on TUBO cell growth in vivo was evaluated after injecting subcutaneously into BALB/c mice anti-miR-135b (**C**; continuous black line, n = 11) or

miR-135b-over (**D**; continuous black line, n = 7). In each experiment TUBO cells were also transfected with negative scrambled anti-miR (**C**; dotted black line, n = 11) and a scrambled mimic (**D**; dotted black line, n = 5). Data are expressed as tumor incidence; differences were analyzed by the log-rank (Mantel-Cox) test.

Figure 4. miR-135b expression is significantly higher in mammospheres as compared to differentiated epithelial TUBO cells miR-135b and is involved in cancer stem cell (CSC) self-renewal. (**A**) FACS analysis of Sca-1, Thy1.1 and Nanog stem cell markers on TUBO, P1 and P2 mammospheres. Data are expressed as means ± SEM of the % of positive cells. Two-tailed Student's t test was used for comparisons between P1 or P2 mammospheres versus TUBO cells (* $P = 0.02$; ** $P = 0.002$; *** $P = 0.0009$). (**B**) miR-135b level in P1 and P2 measured by qPCR and expressed as $2^{-\Delta\Delta Ct}$ normalized to TUBO cells grown in mammosphere medium. Two-tailed Student's t test was used for comparisons (** $P = 0.003$). (**C**) Sphere generation assay 5 days after transfection of P1 derived cells with anti-miR135b or scrambled antagomir. Data are expressed as mammosphere number per 10^3 plated cells. Two-tailed Student's t test was used for comparisons (* $P = 0.01$). (**D**) FACS analysis of Sca-1, Thy1.1 and Nanog stem cell markers on P1 derived cells 24 hours after transfection with anti-miR135b or scrambled antagomir. Data are expressed as means ± SEM of the % of positive cells. Two-tailed Student's t test was used for comparisons between scrambled and miR-135b antagomir transfected P1 derived cells (** P = 0.004).

Figure 5. miR-135b expression significantly enhances anchorage-independent growth in vitro and metastasis formation in vivo. TUBO cells were transfected with specific anti-miR-135b (**A, C**: black bars) or miR-135b mimic (**B, D**: black bars) or their scrambled controls (white bars). Results are shown as mean ± SEM of one out of three independent experiments. Two-tailed Student's t test was used for comparisons. (**A, B**) TUBO cells ability to grow in soft agar and form colonies was evaluated 15 days after down-regulation (**A**) or over-expression (**B**) of miR-135b. Three independent

experiments were performed in triplicate and a representative one is shown. (**C, D**) Lung micrometastasis formation was evaluated 20 days after tail vein injection of transfected TUBO cells in BALB/c mice (4 to 5 mice for each group) on haematoxylin & eosin-stained total lungs sections.

Figure 6. miR-135b downregulates MID1 and MTCH2 target genes. (**A**) Luciferase assays performed on TUBO cells cotransfetced with reporter constructs containing the 3'UTR of the indicated genes cloned downstream of the luciferase coding sequence, together with anti-miR-135b (black bars) or scrambled anti-miR (white bars). Results were calculated as fold changes and are shown as mean ± SEM of firefly luciferase activity relative to controls, normalized on renilla luciferase activity. Two-tailed Student's t test was used for comparisons (* $P = 0.03$). Three independent experiments were performed in triplicate and a representative one is shown. (**B**) MID1 and MTCH2 mRNA levels measured by qPCR in TUBO cells 72 after anti-miR-135b (black bars) or scrambled anti-miR (white bars) transfection. Results were calculated as fold changes (mean ± SEM) relative to scrambled, normalized on β-actin. Two-tailed Student's t test was used for comparisons (** $P = 0.001$; * $P = 0.03$). (**C**) MID1 and MTCH2 protein levels measured by Western blot in TUBO cells transfected with anti-miR-135b (left panels), miR-135b mimic (right panels) or their scrambled controls. The percentage indicated on the right refers to protein modulations. (**D**) MID1 and MTCH2 mRNA levels measured by qPCR in the mammary tissue from 6-week-old (wk6.neu, white bars) and 19-week-old (wk19.neu, black bars) BALB-neuT mice. Results were calculated as fold changes (mean ± SEM) relative to wk6.neu, normalized on β-actin. For all data two-tailed Student's t test was used for comparisons (*** $P = 0.0002$; * $P = 0.02$).

Figure 7. miR-135b prometastatic effect is mediated by MID1 and MTCH2. Number of soft agar colonies generated from TUBO cells transfected with miR-135b insensitive MID1 (MID1 ins), MTCH2 (MTCH2 ins) or the empty vector (as control) and then with miR-135b mimic. Three independent experiments were performed in triplicate and a representative one is shown. Two-tailed

Student’s t test was used to compare each experimental condition with that of miR-135b over-expressing TUBO cells transfected also with empty plasmid (* $P = 0.04$).

References

1. Jemal A, Siegel R, Xu J, Ward E: Cancer statistics, 2010, CA Cancer J Clin 2010, 60:277-300

2. Galvao ER, Martins LM, Ibiapina JO, Andrade HM, Monte SJ: Breast cancer proteomics: a review for clinicians, J Cancer Res Clin Oncol 2011, 137:915-925

3. Gupta GP, Massague J: Cancer metastasis: building a framework, Cell 2006, 127:679-695

4. Nguyen DX, Bos PD, Massague J: Metastasis: from dissemination to organ-specific colonization, Nat Rev Cancer 2009, 9:274-284

5. Valastyan S, Weinberg RA: Tumor metastasis: molecular insights and evolving paradigms, Cell 2011, 147:275-292

6. Nair VS, Maeda LS, Ioannidis JP: Clinical outcome prediction by microRNAs in human cancer: a systematic review, J Natl Cancer Inst 2012, 104:528-540

7. Tavazoie SF, Alarcon C, Oskarsson T, Padua D, Wang Q, Bos PD, Gerald WL, Massague J: Endogenous human microRNAs that suppress breast cancer metastasis, Nature 2008, 451:147-152

8. Zhang J, Ma L: MicroRNA control of epithelial-mesenchymal transition and metastasis, Cancer Metastasis Rev 2012,

9. Bockmeyer CL, Christgen M, Muller M, Fischer S, Ahrens P, Langer F, Kreipe H, Lehmann U: MicroRNA profiles of healthy basal and luminal mammary epithelial cells are distinct and reflected in different breast cancer subtypes, Breast Cancer Res Treat 2011, 130:735-745

10. Blenkiron C, Goldstein LD, Thorne NP, Spiteri I, Chin SF, Dunning MJ, Barbosa-Morais NL, Teschendorff AE, Green AR, Ellis IO, Tavare S, Caldas C, Miska EA: MicroRNA expression profiling of human breast cancer identifies new markers of tumor subtype, Genome Biol 2007, 8:R214

11. Adams BD, Guttilla IK, White BA: Involvement of microRNAs in breast cancer, Semin Reprod Med 2008, 26:522-536

12. Enerly E, Steinfeld I, Kleivi K, Leivonen SK, Aure MR, Russnes HG, Ronneberg JA, Johnsen H, Navon R, Rodland E, Makela R, Naume B, Perala M, Kallioniemi O, Kristensen VN, Yakhini Z, Borresen-Dale AL: miRNA-mRNA integrated analysis reveals roles for miRNAs in primary breast tumors, PLoS One 2011, 6:e16915

13. Lowery AJ, Miller N, Devaney A, McNeill RE, Davoren PA, Lemetre C, Benes V, Schmidt S, Blake J, Ball G, Kerin MJ: MicroRNA signatures predict oestrogen receptor, progesterone receptor and HER2/neu receptor status in breast cancer, Breast Cancer Res 2009, 11:R27

14. Iorio MV, Ferracin M, Liu CG, Veronese A, Spizzo R, Sabbioni S, Magri E, Pedriali M, Fabbri M, Campiglio M, Menard S, Palazzo JP, Rosenberg A, Musiani P, Volinia S, Nenci I, Calin GA, Querzoli P, Negrini M, Croce CM: MicroRNA gene expression deregulation in human breast cancer, Cancer Res 2005, 65:7065-7070

15. Sachdeva M, Mo YY: MicroRNA-145 suppresses cell invasion and metastasis by directly targeting mucin 1, Cancer Res 2010, 70:378-387

16. Png KJ, Yoshida M, Zhang XH, Shu W, Lee H, Rimner A, Chan TA, Comen E, Andrade VP, Kim SW, King TA, Hudis CA, Norton L, Hicks J, Massague J, Tavazoie SF: MicroRNA-335 inhibits tumor reinitiation and is silenced through genetic and epigenetic mechanisms in human breast cancer, Genes Dev 2011, 25:226-231

17. Zhu N, Zhang D, Xie H, Zhou Z, Chen H, Hu T, Bai Y, Shen Y, Yuan W, Jing Q, Qin Y: Endothelial-specific intron-derived miR-126 is down-regulated in human breast cancer and targets both VEGFA and PIK3R2, Mol Cell Biochem 2011, 351:157-164

18. Ma L: Role of miR-10b in breast cancer metastasis, Breast Cancer Res 2010, 12:210

19. Song B, Wang C, Liu J, Wang X, Lv L, Wei L, Xie L, Zheng Y, Song X: MicroRNA-21 regulates breast cancer invasion partly by targeting tissue inhibitor of metalloproteinase 3 expression, J Exp Clin Cancer Res 2010, 29:29

20. Rothe F, Ignatiadis M, Chaboteaux C, Haibe-Kains B, Kheddoumi N, Majjaj S, Badran B, Fayyad-Kazan H, Desmedt C, Harris AL, Piccart M, Sotiriou C: Global microRNA expression profiling identifies MiR-210 associated with tumor proliferation, invasion and poor clinical outcome in breast cancer, PLoS One 2011, 6:e20980

21. Buffa FM, Camps C, Winchester L, Snell CE, Gee HE, Sheldon H, Taylor M, Harris AL, Ragoussis J: microRNA-associated progression pathways and potential therapeutic targets identified by integrated mRNA and microRNA expression profiling in breast cancer, Cancer Res 2011, 71:5635-5645

22. Andorfer CA, Necela BM, Thompson EA, Perez EA: MicroRNA signatures: clinical biomarkers for the diagnosis and treatment of breast cancer, Trends Mol Med 2011, 17:313-319

23. Cavallo F, Offringa R, van der Burg SH, Forni G, Melief CJ: Vaccination for treatment and prevention of cancer in animal models, Adv Immunol 2006, 90:175-213

24. Quaglino E, Mastini C, Forni G, Cavallo F: ErbB2 transgenic mice: a tool for investigation of the immune prevention and treatment of mammary carcinomas, Curr Protoc Immunol 2008, Chapter 20:Unit 20 29 21-20 29-10

25. Husemann Y, Geigl JB, Schubert F, Musiani P, Meyer M, Burghart E, Forni G, Eils R, Fehm T, Riethmuller G, Klein CA: Systemic spread is an early step in breast cancer, Cancer Cell 2008, 13:58-68

26. Astolfi A, Landuzzi L, Nicoletti G, De Giovanni C, Croci S, Palladini A, Ferrini S, Iezzi M, Musiani P, Cavallo F, Forni G, Nanni P, Lollini PL: Gene expression analysis of immune-mediated arrest of tumorigenesis in a transgenic mouse model of HER-2/neu-positive basal-like mammary carcinoma, Am J Pathol 2005, 166:1205-1216

27. Quaglino E, Rolla S, Iezzi M, Spadaro M, Musiani P, De Giovanni C, Lollini PL, Lanzardo S, Forni G, Sanges R, Crispi S, De Luca P, Calogero R, Cavallo F: Concordant morphologic and gene expression data show that a vaccine halts HER-2/neu preneoplastic lesions, J Clin Invest 2004, 113:709-717

28. Boggio K, Nicoletti G, Di Carlo E, Cavallo F, Landuzzi L, Melani C, Giovarelli M, Rossi I, Nanni P, De Giovanni C, Bouchard P, Wolf S, Modesti A, Musiani P, Lollini PL, Colombo MP, Forni G: Interleukin 12-mediated prevention of spontaneous mammary adenocarcinomas in two lines of Her-2/neu transgenic mice, J Exp Med 1998, 188:589-596

29. Workman P, Aboagye EO, Balkwill F, Balmain A, Bruder G, Chaplin DJ, Double JA, Everitt J, Farningham DA, Glennie MJ, Kelland LR, Robinson V, Stratford IJ, Tozer GM, Watson S, Wedge SR, Eccles SA: Guidelines for the welfare and use of animals in cancer research, Br J Cancer 2010, 102:1555-1577

30. Rovero S, Boggio K, Di Carlo E, Amici A, Quaglino E, Porcedda P, Musiani P, Forni G: Insertion of the DNA for the 163-171 peptide of IL1beta enables a DNA vaccine encoding p185(neu) to inhibit mammary carcinogenesis in Her-2/neu transgenic BALB/c mice, Gene Ther 2001, 8:447-452

31. Nanni P, de Giovanni C, Lollini PL, Nicoletti G, Prodi G: TS/A: a new metastasizing cell line from a BALB/c spontaneous mammary adenocarcinoma, Clin Exp Metastasis 1983, 1:373-380

32. Grange C, Lanzardo S, Cavallo F, Camussi G, Bussolati B: Sca-1 identifies the tumor-initiating cells in mammary tumors of BALB-neuT transgenic mice, Neoplasia 2008, 10:1433-1443

33. Bookout AL, Mangelsdorf DJ: Quantitative real-time PCR protocol for analysis of nuclear receptor signaling pathways, Nucl Recept Signal 2003, 1:e012

34. Gentleman RC, Carey VJ, Bates DM, Bolstad B, Dettling M, Dudoit S, Ellis B, Gautier L, Ge Y, Gentry J, Hornik K, Hothorn T, Huber W, Iacus S, Irizarry R, Leisch F, Li C, Maechler M, Rossini AJ, Sawitzki G, Smith C, Smyth G, Tierney L, Yang JY, Zhang J: Bioconductor: open software development for computational biology and bioinformatics, Genome Biol 2004, 5:R80

35. Breitling R, Armengaud P, Amtmann A, Herzyk P: Rank products: a simple, yet powerful, new method to detect differentially regulated genes in replicated microarray experiments, FEBS Lett 2004, 573:83-92

36. Sasson A, Michael TP: Filtering error from SOLiD Output, Bioinformatics 2010, 26:849-850

37. Rumble SM, Lacroute P, Dalca AV, Fiume M, Sidow A, Brudno M: SHRiMP: accurate mapping of short color-space reads, PLoS Comput Biol 2009, 5:e1000386

38. Sanges R, Cordero F, Calogero RA: oneChannelGUI: a graphical interface to Bioconductor tools, designed for life scientists who are not familiar with R language, Bioinformatics 2007, 23:3406-3408

39. Robinson MD, Smyth GK: Small-sample estimation of negative binomial dispersion, with applications to SAGE data, Biostatistics 2008, 9:321-332

40. Perou CM, Sorlie T, Eisen MB, van de Rijn M, Jeffrey SS, Rees CA, Pollack JR, Ross DT, Johnsen H, Akslen LA, Fluge O, Pergamenschikov A, Williams C, Zhu SX, Lonning PE, Borresen-Dale AL, Brown PO, Botstein D: Molecular portraits of human breast tumours, Nature 2000, 406:747-752

41. Betel D, Koppal A, Agius P, Sander C, Leslie C: Comprehensive modeling of microRNA targets predicts functional non-conserved and non-canonical sites, Genome Biol 2010, 11:R90

42. Gilli F, Lindberg RL, Valentino P, Marnetto F, Malucchi S, Sala A, Capobianco M, di Sapio A, Sperli F, Kappos L, Calogero RA, Bertolotto A: Learning from nature: pregnancy changes the expression of inflammation-related genes in patients with multiple sclerosis, PLoS One 2010, 5:e8962

43. Smyth GK: Linear models and empirical bayes methods for assessing differential expression in microarray experiments, Stat Appl Genet Mol Biol 2004, 3:Article3

44. Calogero RA, Quaglino E, Saviozzi S, Forni G, Cavallo F: Oncoantigens as anti-tumor vaccination targets: the chance of a lucky strike?, Cancer Immunol Immunother 2008, 57:1685-1694

45. Cho RW, Wang X, Diehn M, Shedden K, Chen GY, Sherlock G, Gurney A, Lewicki J, Clarke MF: Isolation and molecular characterization of cancer stem cells in MMTV-Wnt-1 murine breast tumors, Stem Cells 2008, 26:364-371

46. Jeter CR, Liu B, Liu X, Chen X, Liu C, Calhoun-Davis T, Repass J, Zaehres H, Shen JJ, Tang DG: NANOG promotes cancer stem cell characteristics and prostate cancer resistance to androgen deprivation, Oncogene 30:3833-3845

47. Hao JM, Chen JZ, Sui HM, Si-Ma XQ, Li GQ, Liu C, Li JL, Ding YQ, Li JM: A five-gene signature as a potential predictor of metastasis and survival in colorectal cancer, J Pathol 2010, 220:475-489

48. Yu K, Ganesan K, Tan LK, Laban M, Wu J, Zhao XD, Li H, Leung CH, Zhu Y, Wei CL, Hooi SC, Miller L, Tan P: A precisely regulated gene expression cassette potently modulates metastasis and survival in multiple solid cancers, PLoS Genet 2008, 4:e1000129

49. Klein U, Dalla-Favera R: New insights into the pathogenesis of chronic lymphocytic leukemia, Semin Cancer Biol 2010, 20:377-383

50. Hurst DR, Edmonds MD, Welch DR: Metastamir: the field of metastasis-regulatory microRNA is spreading, Cancer Res 2009, 69:7495-7498

51. Polyak K, Weinberg RA: Transitions between epithelial and mesenchymal states: acquisition of malignant and stem cell traits, Nat Rev Cancer 2009, 9:265-273

52. Urbich C, Kuehbacher A, Dimmeler S: Role of microRNAs in vascular diseases, inflammation, and angiogenesis, Cardiovasc Res 2008, 79:581-588

53. Astolfi A, Rolla S, Nanni P, Quaglino E, De Giovanni C, Iezzi M, Musiani P, Forni G, Lollini PL, Cavallo F, Calogero RA: Immune prevention of mammary carcinogenesis in HER-2/neu transgenic mice: a microarray scenario, Cancer Immunol Immunother 2005, 54:599-610

54. Cavallo F, Calogero RA, Forni G: Are oncoantigens suitable targets for anti-tumour therapy?, Nat Rev Cancer 2007, 7:707-713

55. Calogero RA, Quaglino E, Saviozzi S, Forni G, Cavallo F: Oncoantigens as anti-tumor vaccination targets: the chance of a lucky strike?, Cancer Immunol Immunother 2008,

56. Li LN, Zhang HD, Zhi R, Yuan SJ: Down-regulation of some miRNAs by degrading their precursors contributes to anti-cancer effect of mistletoe lectin-I, Br J Pharmacol 2011, 162:349-364

57. Navarro A, Diaz T, Martinez A, Gaya A, Pons A, Gel B, Codony C, Ferrer G, Martinez C, Montserrat E, Monzo M: Regulation of JAK2 by miR-135a: prognostic impact in classic Hodgkin lymphoma, Blood 2009, 114:2945-2951

58. Wang YX, Zhang XY, Zhang BF, Yang CQ, Chen XM, Gao HJ: Initial study of microRNA expression profiles of colonic cancer without lymph node metastasis, J Dig Dis 2010, 11:50-54

59. Vickers MM, Bar J, Gorn-Hondermann I, Yarom N, Daneshmand M, Hanson JE, Addison CL, Asmis TR, Jonker DJ, Maroun J, Lorimer IA, Goss GD, Dimitroulakos J: Stage-dependent differential expression of microRNAs in colorectal cancer: potential role as markers of metastatic disease, Clin Exp Metastasis 2012, 29:123-132

60. Xu XM, Qian JC, Deng ZL, Cai Z, Tang T, Wang P, Zhang KH, Cai JP: Expression of miR-21, miR-31, miR-96 and miR-135b is correlated with the clinical parameters of colorectal cancer, Oncol Lett 2012, 4:339-345

61. Lulla RR, Costa FF, Bischof JM, Chou PM, de FBM, Vanin EF, Soares MB: Identification of Differentially Expressed MicroRNAs in Osteosarcoma, Sarcoma 2011, 2011:732690

62. Costa FF, Bischof JM, Vanin EF, Lulla RR, Wang M, Sredni ST, Rajaram V, Bonaldo Mde F, Wang D, Goldman S, Tomita T, Soares MB: Identification of microRNAs as potential prognostic markers in ependymoma, PLoS One 2011, 6:e25114

63. Liu S, Guo W, Shi J, Li N, Yu X, Xue J, Fu X, Chu K, Lu C, Zhao J, Xie D, Wu M, Cheng S: MicroRNA-135a contributes to the development of portal vein tumor thrombus by promoting metastasis in hepatocellular carcinoma, J Hepatol 2012, 56:389-396

64. Rovero S, Amici A, Di Carlo E, Bei R, Nanni P, Quaglino E, Porcedda P, Boggio K, Smorlesi A, Lollini PL, Landuzzi L, Colombo MP, Giovarelli M, Musiani P, Forni G: DNA vaccination against rat her-2/Neu p185 more effectively inhibits carcinogenesis than transplantable carcinomas in transgenic BALB/c mice, J Immunol 2000, 165:5133-5142

65. Lindow M, Gorodkin J: Principles and limitations of computational microRNA gene and target finding, DNA Cell Biol 2007, 26:339-351

66. Alexiou P, Maragkakis M, Papadopoulos GL, Reczko M, Hatzigeorgiou AG: Lost in translation: an assessment and perspective for computational microRNA target identification, Bioinformatics 2009, 25:3049-3055

67. Aranda-Orgilles B, Aigner J, Kunath M, Lurz R, Schneider R, Schweiger S: Active transport of the ubiquitin ligase MID1 along the microtubules is regulated by protein phosphatase 2A, PLoS One 2008, 3:e3507

68. Leibowitz-Amit R, Tsarfaty G, Abargil Y, Yerushalmi GM, Horev J, Tsarfaty I: Mimp, a mitochondrial carrier homologue, inhibits Met-HGF/SF-induced scattering and tumorigenicity by altering Met-HGF/SF signaling pathways, Cancer Res 2006, 66:8687-8697

69. Zaltsman Y, Shachnai L, Yivgi-Ohana N, Schwarz M, Maryanovich M, Houtkooper RH, Vaz FM, De Leonardis F, Fiermonte G, Palmieri F, Gillissen B, Daniel PT, Jimenez E, Walsh S, Koehler CM, Roy SS, Walter L, Hajnoczky G, Gross A: MTCH2/MIMP is a major facilitator of tBID recruitment to mitochondria, Nat Cell Biol 2010, 12:553-562

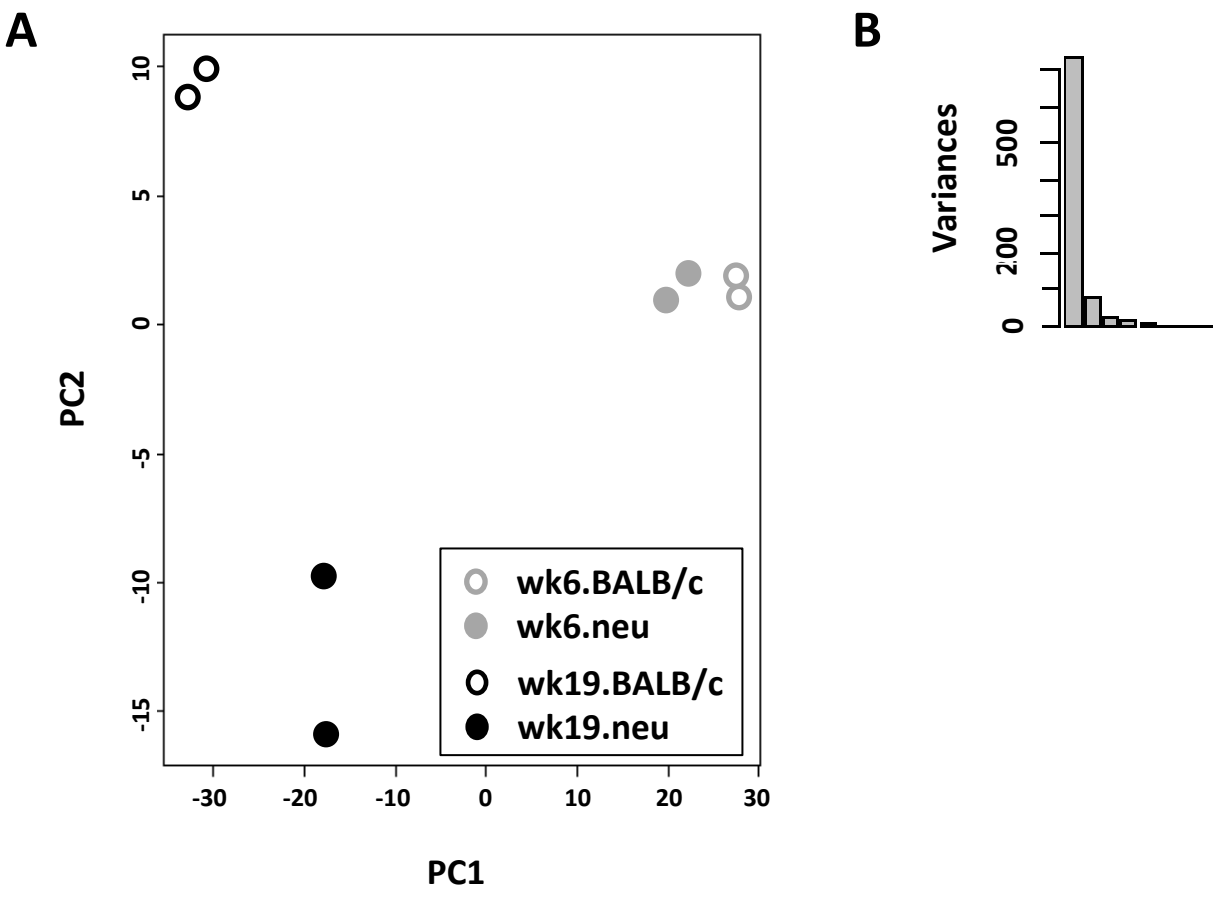

Figure 1, Arigoni et al.

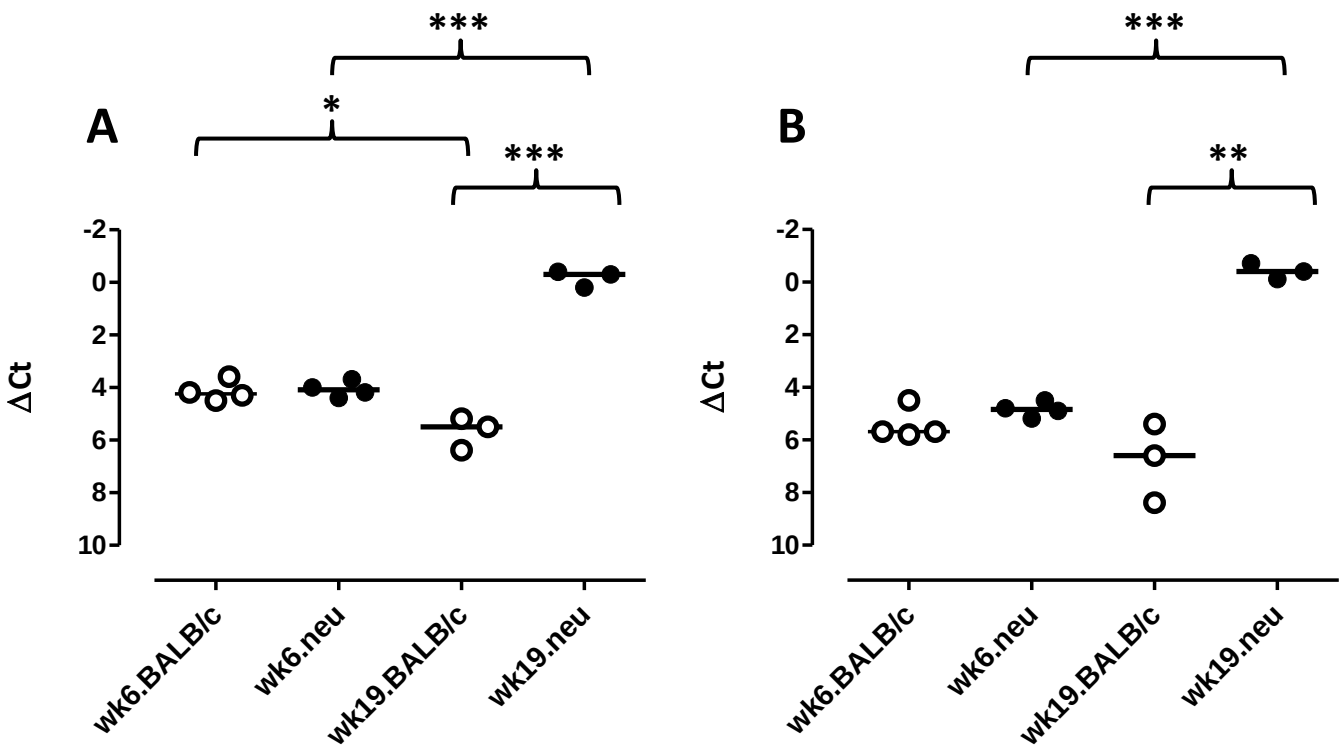

Figure 2, Arigoni et al.

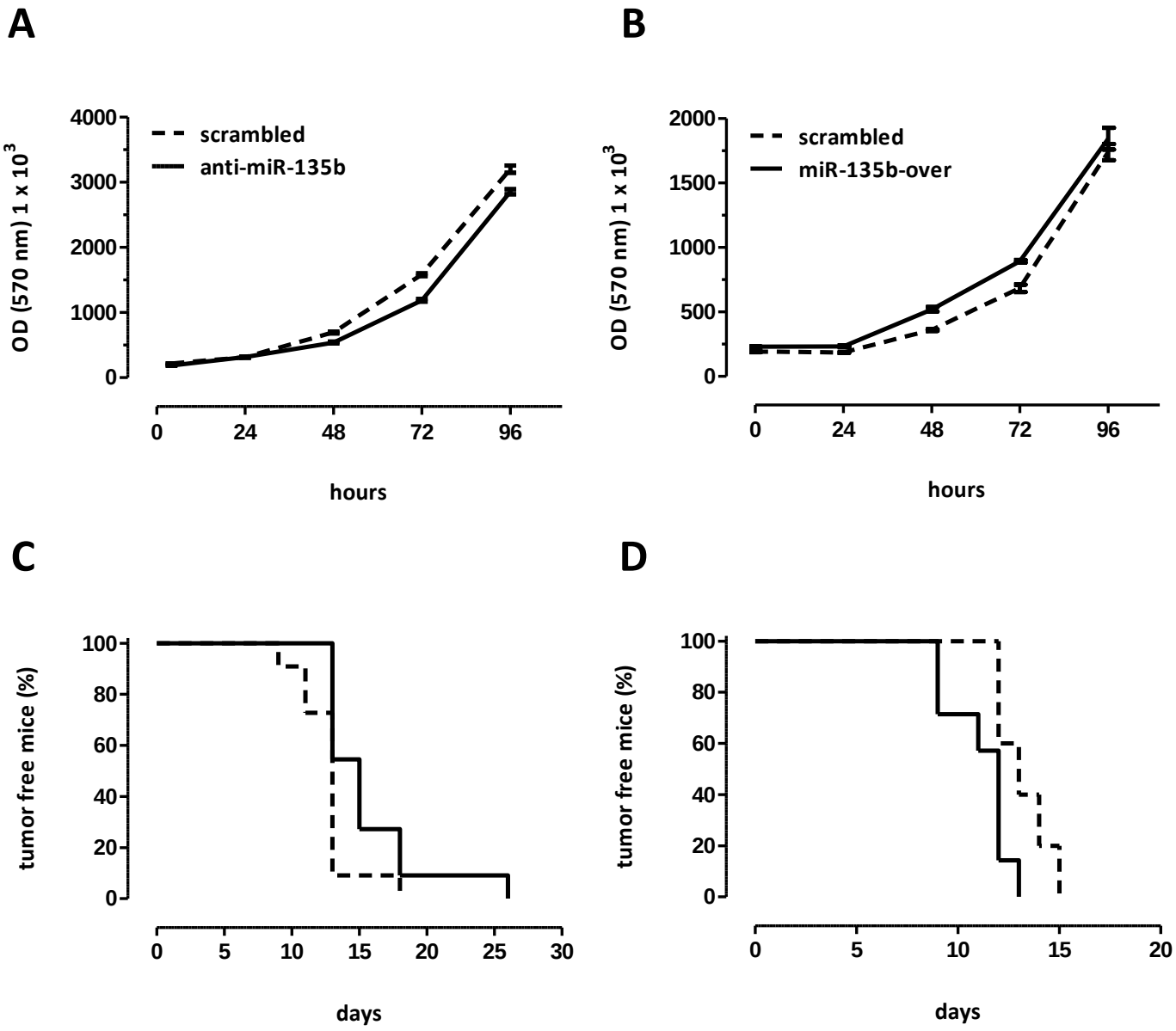

Figure 3, Arigoni et al.

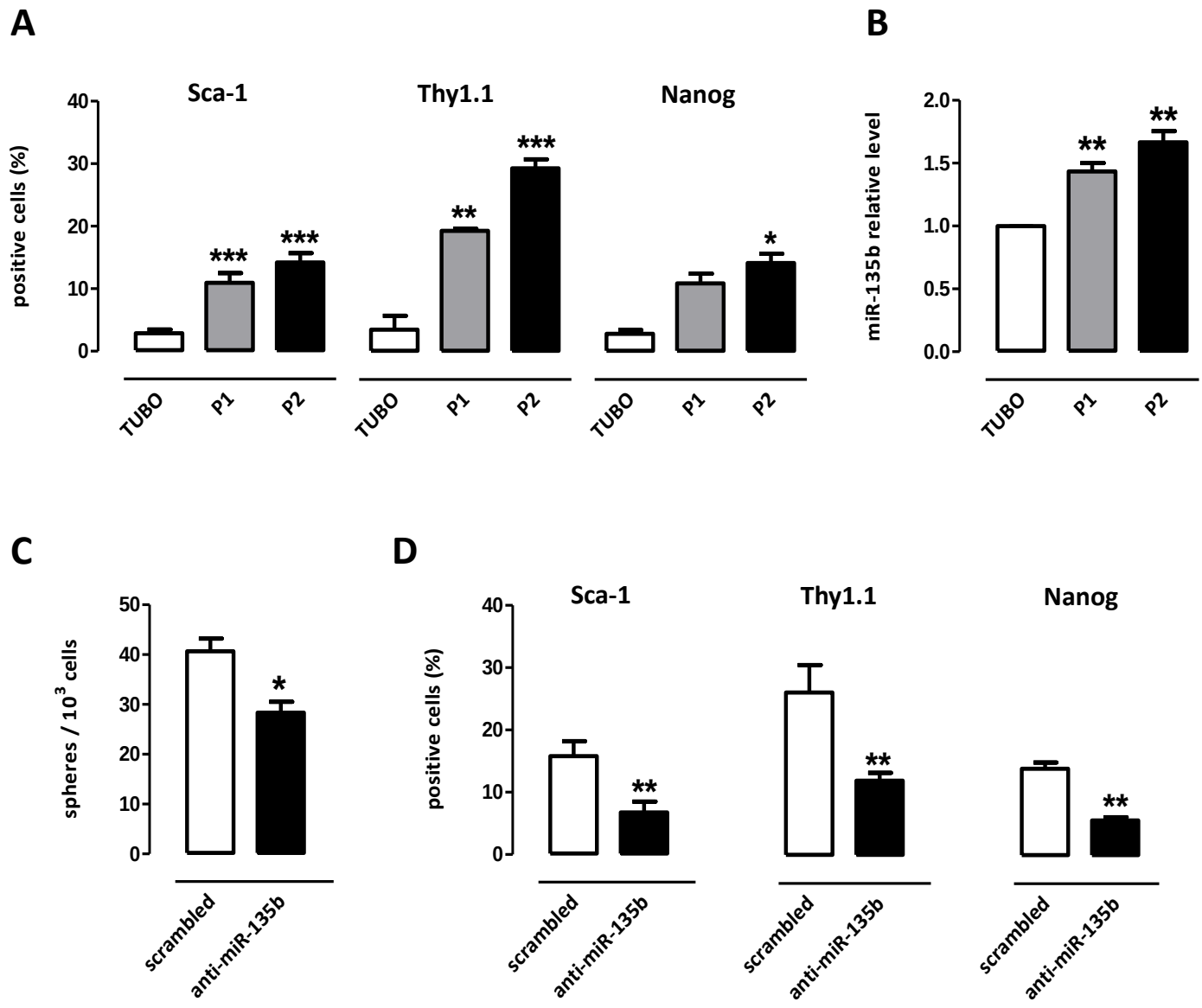

Figure 4, Arigoni et al.

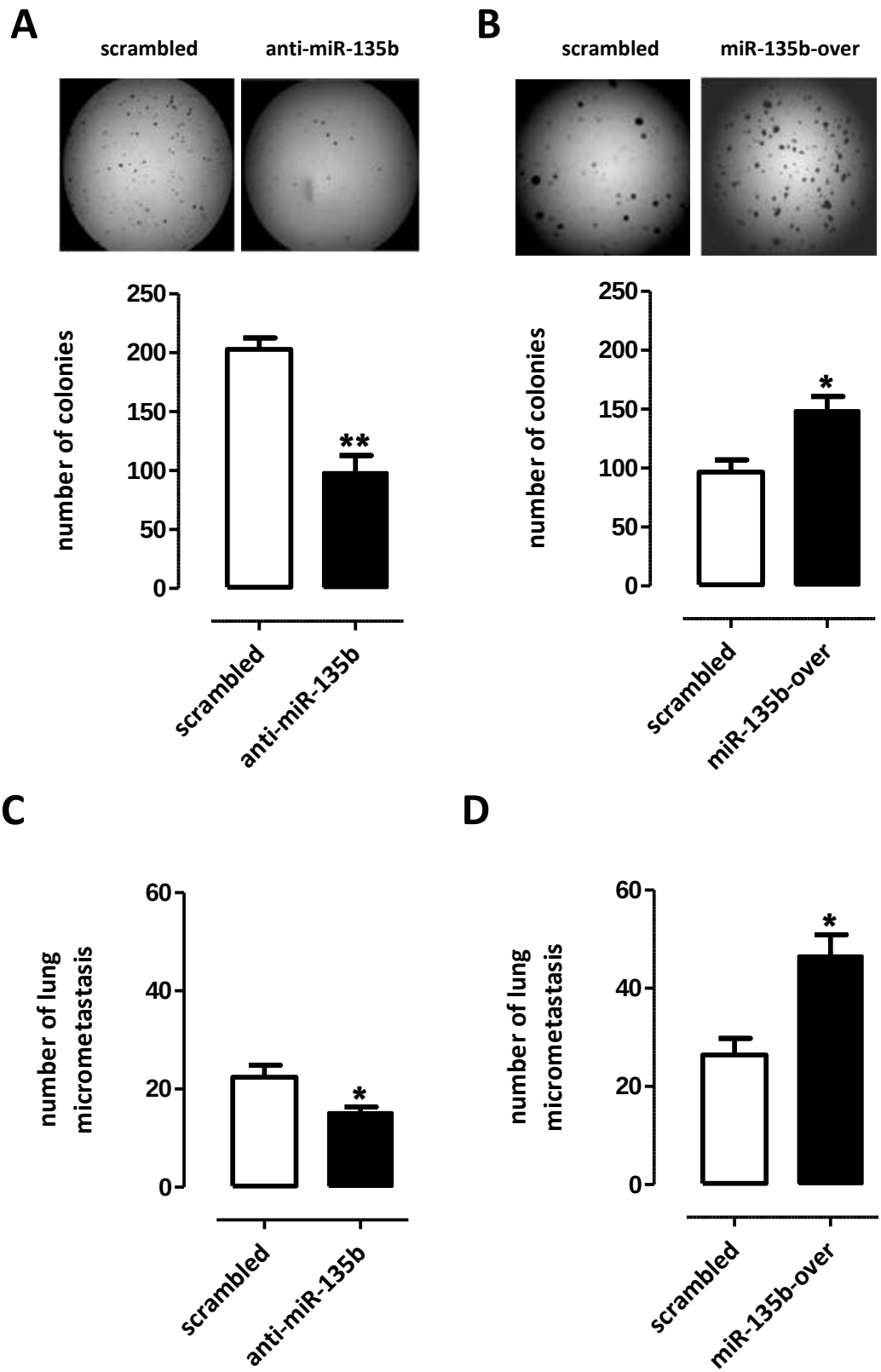

Figure 5, Arigoni et al.

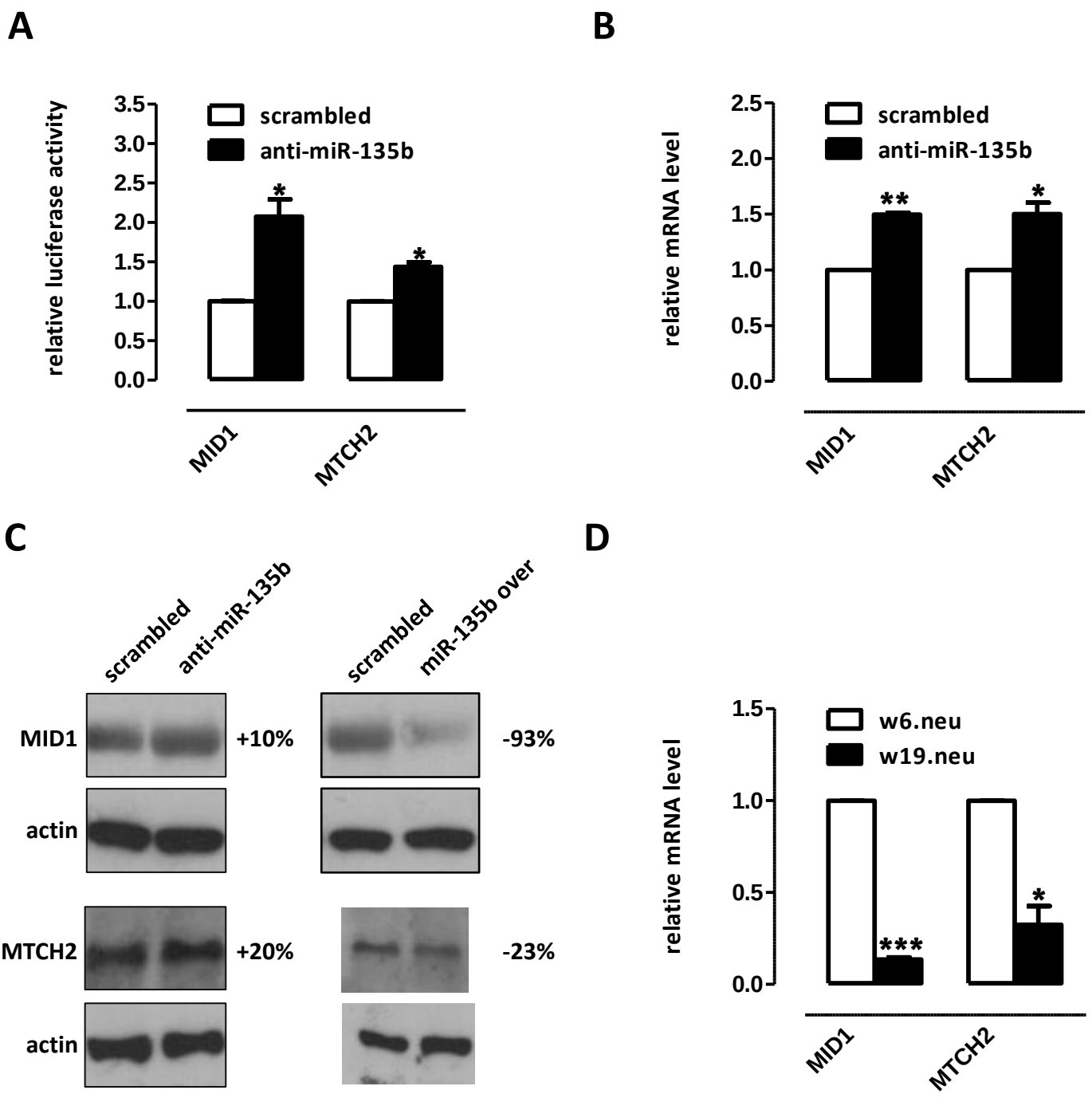

Figure 6, Arigoni et al.

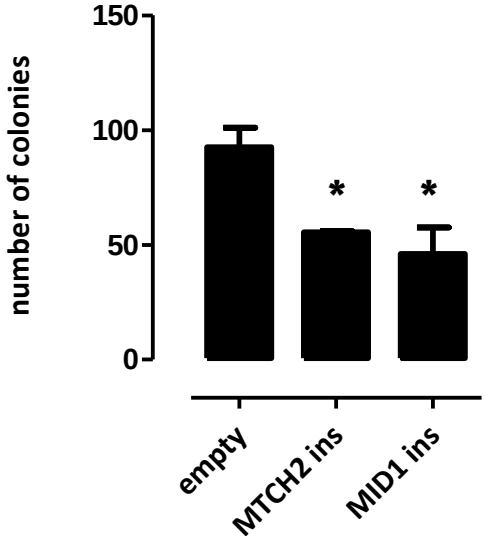

Figure 7, Arigoni et al.